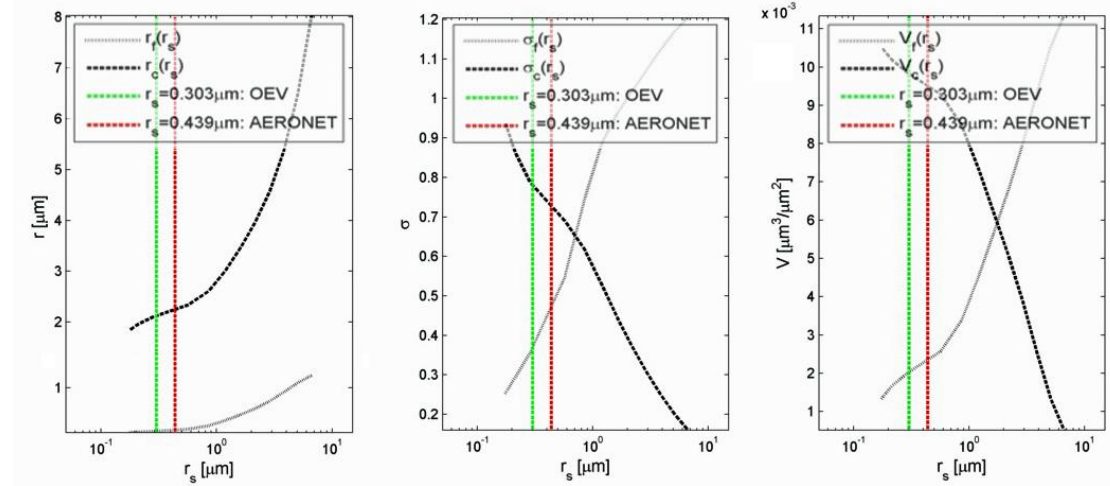


## Supplementary Material

### S1 Sensitivity Analysis

#### S1.1 Dependence of microphysical parameters on $r_s$

In order to assess the impact of changes in the location of the  $r_s$  on the deduction of secondary (derived) microphysical parameters, in Figure S1 we present these parameters as a function of the mode separation point over the range  $0.1 \leq r_s \leq 7 \mu\text{m}$  for the AVSD at Lanai, Hawaii on the 21<sup>st</sup> of January, 2002 interpolated with 2200 points:



**Figure S1.** Sensitivity of the values of secondary (deduced) microphysical parameters on the position of the mode separation point  $r_s$  for AERONET bi-lognormal fits OEV fits to the AVSD of dominant marine (sea salt) aerosol at Lanai, Hawaii on the 21<sup>st</sup> of January, 2002.

The slope of each parameter curve reflects its rate of change with respect to the mode separation point  $r_s$ . In order to quantify this rate of change, we calculated the relative error for each parameter  $\beta(r_s)$  with respect to the AERONET value of the parameter  $\beta(AERONET)$ ,

$$RE[\beta(r_s)] = 1 - \frac{\beta(r_s)}{\beta(AERONET)} \quad (S1)$$

where  $\beta = V_f, V_c, r_f, r_c, \sigma_f$  and  $\sigma_c$ . Table S1 summarizes the results of this analysis for all 4 dominant aerosol type cases.

a) Mineral Dust $r_s$	RE ( $r_f$ ) [%]	RE ( $r_c$ ) [%]	RE ( $\sigma_f$ ) [%]	RE ( $\sigma_c$ ) [%]	RE ( $V_f$ ) [%]	RE ( $V_c$ ) [%]
0.175	47.04	8.76	52.04	-21.51	56.57	-5.68
0.180	46.40	8.58	50.93	-20.92	55.58	-5.58
0.186	45.64	8.36	49.60	-20.25	54.43	-5.46
0.194	44.68	8.09	47.94	-19.46	53.03	-5.32
0.204	43.45	7.77	45.80	-18.50	51.28	-5.14
0.216	42.02	7.41	43.33	-17.47	49.32	-4.94
0.286	32.74	5.45	28.98	-12.22	37.74	-3.77
0.567	-29.18	-5.20	-7.06	9.49	-37.95	3.92
0.858	-86.99	-14.60	-16.10	23.77	-115.86	11.82
1.202	-157.71	-24.24	-23.16	33.30	-211.75	21.56
b) Biomass Burning $r_s$	RE ( $r_f$ ) [%]	RE ( $r_c$ ) [%]	RE ( $\sigma_f$ ) [%]	RE ( $\sigma_c$ ) [%]	RE ( $V_f$ ) [%]	RE ( $V_c$ ) [%]
0.175	23.20	69.00	40.54	-126.02	39.92	-78.34
0.180	21.99	67.28	39.11	-123.79	37.26	-73.08
0.186	20.56	65.05	37.41	-120.77	34.17	-66.98
0.194	18.83	62.00	35.29	-116.41	30.46	-59.66
0.204	16.71	57.64	32.61	-109.81	26.01	-50.88
0.216	14.50	52.25	29.74	-101.13	21.52	-42.02
0.286	6.88	25.80	18.10	-52.51	7.92	-15.18
0.567	0.60	2.23	2.57	-3.31	0.64	-0.81
0.858	-2.43	-4.34	-8.85	8.44	-1.41	3.24
1.202	-6.46	-10.51	-25.08	17.28	-3.59	7.54
c) Urban SO <sub>2</sub> $r_s$	RE ( $r_f$ ) [%]	RE ( $r_c$ ) [%]	RE ( $\sigma_f$ ) [%]	RE ( $\sigma_c$ ) [%]	RE ( $V_f$ ) [%]	RE ( $V_c$ ) [%]
0.175	28.33	78.73	46.17	-113.97	45.54	-159.17
0.180	27.22	77.75	44.82	-113.69	43.14	-150.73
0.186	25.91	76.50	43.21	-113.22	40.36	-140.94
0.194	24.32	74.80	41.21	-112.37	37.03	-129.20
0.204	22.36	72.39	38.68	-110.83	33.00	-115.04
0.216	20.26	69.34	35.89	-108.38	28.82	-100.32
0.286	11.45	48.73	22.96	-83.28	13.30	-45.70
0.567	1.72	5.14	3.52	-9.02	1.31	-3.49
0.858	-0.21	-2.09	-2.63	3.03	-0.08	1.41
1.202	-2.58	-8.01	-11.61	10.31	-1.40	6.06
d) Marine Sea Salt $r_s$	RE ( $r_f$ ) [%]	RE ( $r_c$ ) [%]	RE ( $\sigma_f$ ) [%]	RE ( $\sigma_c$ ) [%]	RE ( $V_f$ ) [%]	RE ( $V_c$ ) [%]
0.175	27.62	18.34	45.34	-29.53	33.14	-5.20
0.180	26.58	17.40	44.06	-27.87	30.59	-4.68
0.186	25.37	16.33	42.54	-25.98	27.69	-4.11
0.194	23.92	15.06	40.66	-23.76	24.29	-3.43
0.204	22.16	13.55	38.30	-21.13	20.28	-2.62
0.216	20.28	11.99	35.69	-18.44	16.19	-1.81
0.286	12.20	6.09	23.13	-8.69	0.79	1.27
0.567	-11.20	-4.14	-17.51	4.66	-28.54	7.14
0.858	-53.69	-16.46	-62.16	15.27	-68.73	15.18
1.202	-118.16	-34.68	-91.68	27.42	-125.65	26.56

**Table S1.** Relative errors (RE) of the microphysical parameters derived with the OEV fit relative to those presented by AERONET over a broad range of values of the mode separation point  $r_s$  considered in the sensitivity analysis described in Section 3.2 for 4 dominant aerosol type cases: a) dust at Banizoumbou, b) biomass burning at Mongu, c) urban sulphate (SO<sub>2</sub>) at Washington-GSFC, and d) marine sea salt at Lanai.

## S1.2 Dependence of microphysical parameters on AOD

It is known that a strong correlation exists between the total aerosol volume concentration and the aerosol load as expressed through the AOD (Sayer et al., 2012). For this reason, in an earlier paper (Dubovik et al., 2002), microphysical parameters obtained by AERONET were expressed as a direct function of the AOD. In order to assess the impact of the OEV fits on this dependence, we present in Figure S2 below the dependence on AOD(1020nm) of parameters calculated with both the AERONET bi-lognormal fit and the OEV fit over a time window of 20 days around the marine aerosol peak (21<sup>st</sup> of January, 2002) at Lanai, Hawaii.

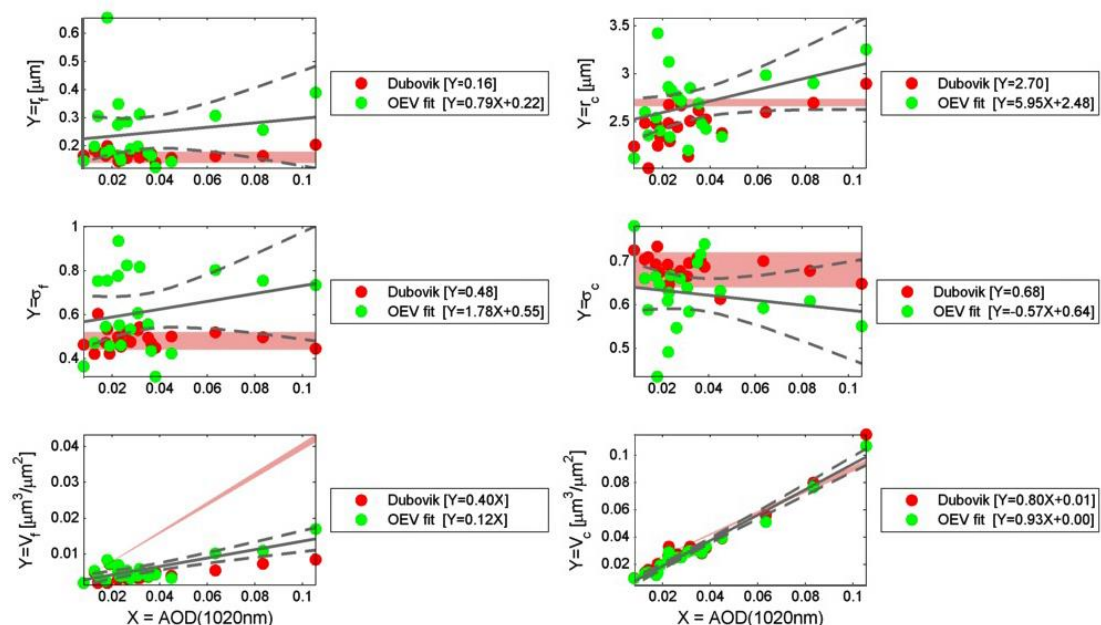


**Figure S2.** Sensitivity to the aerosol load (as measured through the AOD at 1020nm) of the values of secondary microphysical parameters obtained with AERONET bi-lognormal fits and OEV fits to the AVSD of dominant marine (sea salt) aerosol at Lanai, Hawaii during the period: 3<sup>rd</sup> of January to 16<sup>th</sup> of February, 2002. The pink shaded regions are the dependence of the parameters on AOD(1020nm) as quoted by Dubovik et al (2002). The thick grey line is the best fit linear regression to the OEV data with 95% confidence intervals (dotted lines).

## S2 Statistical Assumption Test

At the heart of the hypothesis testing method developed in Section 3.3 is the assumption that adding more modes and therefore model parameters in the nesting procedure does not cause much divergence to occur between the coefficient of determination  $R_d^2$  and the degrees of freedom-adjusted  $R^2$  defined in equations (B4) and (B6) in Appendix B. This is verified below for all of the dominant aerosol type cases. Table S2 shows the calculation of the correction to  $R^2$  resulting from including the degrees-of-freedom adjustment.

a) Mineral Dust	modes	Radj <sup>2</sup>	correction	SSE/SST	R <sup>2</sup>	RE %
AERONET inversion	2	0.913	1.003	0.086	0.914	0.026%
OEV (r <sub>s</sub> ; min s)	2	0.978	1.003	0.021	0.979	0.006%
OEV (r <sub>s</sub> ; max R <sup>2</sup> )	2	0.978	1.003	0.021	0.979	0.006%
OEV (mean r <sub>s</sub> )	2	0.978	1.003	0.021	0.979	0.006%
GMM	1	0.949	1.001	0.051	0.949	0.007%
GMM	2	0.995	1.003	0.005	0.995	0.002%
GMM	3	0.995	1.004	0.005	0.995	0.002%
GMM	4	0.998	1.005	0.002	0.998	0.001%
GMM	5	0.996	1.007	0.004	0.996	0.003%
GMM	6	0.996	1.008	0.004	0.996	0.003%
b) Biomass Burning	modes	Radj <sup>2</sup>	correction	SSE/SST	R <sup>2</sup>	RE %
AERONET inversion	2	0.983	1.003	0.017	0.983	0.005%
OEV (r <sub>s</sub> ; min s)	2	0.985	1.003	0.015	0.985	0.004%
OEV (r <sub>s</sub> ; max R <sup>2</sup> )	2	0.985	1.003	0.015	0.985	0.004%
OEV (mean r <sub>s</sub> )	2	0.985	1.003	0.015	0.985	0.004%
GMM	1	0.804	1.001	0.196	0.804	0.033%
GMM	2	0.993	1.003	0.007	0.993	0.002%
GMM	3	0.998	1.004	0.002	0.998	0.001%
GMM	4	0.998	1.005	0.002	0.998	0.001%
GMM	5	0.998	1.007	0.002	0.998	0.001%
GMM	6	0.998	1.008	0.002	0.998	0.001%
c) Urban SO <sub>2</sub>	modes	Radj <sup>2</sup>	correction	SSE/SST	R <sup>2</sup>	RE %
AERONET inversion	2	0.982	1.003	0.018	0.982	0.005%
OEV (r <sub>s</sub> ; min s)	2	0.987	1.003	0.013	0.987	0.003%
OEV (r <sub>s</sub> ; max R <sup>2</sup> )	2	0.987	1.003	0.013	0.987	0.003%
OEV (mean r <sub>s</sub> )	2	0.987	1.003	0.013	0.987	0.003%
GMM	1	0.919	1.001	0.081	0.919	0.012%
GMM	2	0.954	1.003	0.046	0.954	0.013%
GMM	3	0.999	1.004	0.001	0.999	0.000%
GMM	4	1.000	1.005	0.000	1.000	0.000%
GMM	5	1.000	1.007	0.000	1.000	0.000%
GMM	6	1.000	1.008	0.000	1.000	0.000%
d) Marine Sea Salt	modes	R <sup>2</sup>	correction	SSE/SST	Rd <sup>2</sup>	RE %
AERONET inversion	2	0.885	1.003	0.115	0.885	0.036%
OEV (r <sub>s</sub> ; min s)	2	0.893	1.003	0.107	0.893	0.033%
OEV (r <sub>s</sub> ; max R <sup>2</sup> )	2	0.894	1.003	0.106	0.894	0.032%
OEV (mean r <sub>s</sub> )	2	0.894	1.003	0.106	0.894	0.032%
GMM	1	0.777	1.001	0.223	0.777	0.039%
GMM	2	0.819	1.003	0.181	0.819	0.060%
GMM	3	0.998	1.004	0.002	0.998	0.001%
GMM	4	0.993	1.005	0.007	0.993	0.004%
GMM	5	1.000	1.007	0.000	1.000	0.000%
GMM	6	1.000	1.008	0.000	1.000	0.000%

**Table S2.** Comparison of the relative error (RE) in percent resulting from not including the degrees-of-freedom adjustment in the calculation of  $R^2$  for each of the 4 dominant aerosol type cases (as in Table S1). The calculation is performed for the reconstructed AERONET Level 2.0 Version 2 bi-lognormal fit, the OEV bi-lognormal fits and the GMM fits with 1-6 modes. The first four rows in each case correspond to the AERONET bi-lognormal fit and the three OEV bi-lognormal fits.

The percentage relative error (RE) is very small for both bi-lognormal fits and for GMMs containing 1-6 modes reaching a maximum value of RE=0.060% for the 2-modal GMM fit to the dominant marine aerosol AVSD. Propagating this error into the square root of  $R^2$  (the proxy for Pearson's  $\rho$ ), its effect is at the 4th decimal place and does not impinge on the results of the hypothesis testing procedure at the 95% level.

### **S3 Inter-model Comparison**

In Table S3, we collect together the results of fitting the AVSD with the OEV and GMM methods. For these fits, the volume concentrations [V1,V2], the geometric mean radii [r1,r2] and standard deviations [ $\sigma$ 1, $\sigma$ 2] correspond to those of the traditional fine and coarse modes. For the fits resulting from the GMM method with 1-6 modes, the microphysical parameters (mode volume concentrations [V1...V6] and geometric mean radii [r1...r6]) have been sorted by increasing geometric mean radius for ease of interpretation, i.e. so that it is possible to associate particle size with contribution to the total volume concentration.

a) Mineral Dust	$r_s$	modes	b	s	$R^2$	V	V1	V2	V3	V4	V5	V6	r1	r2	r3	r4	r5	r6
AERONET																		
inversion	0.439	2	4.94E-05	0.020	0.913	0.311	0.029	0.282					0.195	1.732				
OEV (min $s$ )	0.847	2	3.84E-05	0.010	0.978	0.310	0.061	0.249					0.361	1.980				
OEV (max $R^2$ )	0.854	2	3.81E-05	0.010	0.978	0.310	0.061	0.249					0.363	1.983				
OEV (mean)	0.852	2	3.83E-05	0.010	0.978	0.310	0.061	0.249					0.361	1.981				
GMM		1	0.010	0.017	0.949	0.256	0.256						1.905					
GMM		2	0.002	0.005	0.995	0.301	0.131	0.170					1.074	2.009				
GMM		3	0.002	0.005	0.995	0.301	0.000	0.131	0.170				0.354	1.073	2.009			
GMM		4	0.001	0.003	0.998	0.306	0.029	0.062	0.004	0.212			0.645	0.677	1.632	1.972		
GMM		5	0.002	0.004	0.996	0.301	0.000	0.128	0.022	0.143	0.008		0.403	1.066	1.661	2.078	2.359	
GMM		6	0.002	0.004	0.996	0.301	0.000	0.128	0.022	0.143	0.008	0.000	0.290	1.065	1.661	2.078	2.358	2.406
b) Biomass Burning																		
AERONET																		
inversion	0.648	2	5.85E-05	0.003	0.983	0.112	0.074	0.038					0.160	3.385				
OEV (min $s$ )	0.551	2	9.05E-05	0.002	0.985	0.112	0.074	0.038					0.159	3.293				
OEV (max $R^2$ )	0.541	2	9.14E-05	0.002	0.985	0.112	0.074	0.038					0.158	3.283				
OEV (mean)	0.546	2	9.10E-05	0.002	0.985	0.112	0.074	0.038					0.158	3.288				
GMM		1	0.007	0.010	0.804	0.073	0.073						0.156					
GMM		2	0.000	0.002	0.993	0.109	0.073	0.036					0.156	3.753				
GMM		3	0.000	0.001	0.998	0.111	0.071	0.013	0.027				0.154	1.529	4.172			
GMM		4	0.000	0.001	0.998	0.111	0.000	0.069	0.013	0.027			0.101	0.156	1.499	4.163		
GMM		5	0.000	0.001	0.998	0.111	0.000	0.001	0.070	0.013	0.027		0.081	0.103	0.156	1.496	4.162	
GMM		6	0.000	0.001	0.998	0.111	0.000	0.001	0.000	0.069	0.013	0.027	0.083	0.105	0.138	0.156	1.501	4.162
c) Urban SO <sub>2</sub>																		
AERONET																		
inversion	0.756	2	9.54E-06	0.002	0.982	0.056	0.044	0.013					0.172	3.163				
OEV (min $s$ )	0.531	2	3.72E-05	0.001	0.987	0.056	0.043	0.013					0.168	2.945				
OEV (max $R^2$ )	0.524	2	3.75E-05	0.001	0.987	0.056	0.043	0.013					0.168	2.932				
OEV (mean)	0.528	2	3.75E-05	0.001	0.987	0.056	0.043	0.013					0.168	2.935				
GMM		1	0.002	0.004	0.919	0.044	0.044						0.163					
GMM		2	-0.001	0.002	0.954	0.062	0.049	0.013					0.152	3.174				
GMM		3	0.000	0.000	0.999	0.056	0.015	0.028	0.013				0.130	0.195	3.168			
GMM		4	0.000	0.000	1.000	0.056	0.010	0.029	0.005	0.013			0.119	0.176	0.304	3.188		
GMM		5	0.000	0.000	1.000	0.056	0.024	0.017	0.002	0.001	0.013		0.131	0.214	0.349	0.524	3.187	
GMM		6	0.000	0.000	1.000	0.056	0.020	0.021	0.003	0.000	0.004	0.008	0.127	0.203	0.359	0.861	2.008	4.346
d) Marine Sea Salt																		
AERONET																		
inversion	0.439	2	-1.58E-05	0.001	0.885	0.012	0.002	0.010					0.166	2.244				
OEV (min $s$ )	0.290	2	1.13E-05	0.001	0.893	0.012	0.002	0.010					0.146	2.112				
OEV (max $R^2$ )	0.315	2	1.06E-05	0.001	0.894	0.012	0.002	0.010					0.150	2.141				
OEV (mean)	0.303	2	1.10E-05	0.001	0.894	0.012	0.002	0.010					0.148	2.123				
GMM		1	0.000	0.001	0.777	0.010	0.010						2.253					
GMM		2	0.000	0.001	0.819	0.010	0.002	0.008					0.147	1.883				
GMM		3	0.000	0.000	0.998	0.012	0.002	0.006	0.004				0.152	1.350	4.103			
GMM		4	0.000	0.000	0.993	0.012	0.002	0.005	0.000	0.004			0.147	1.245	2.375	4.111		
GMM		5	0.000	0.000	1.000	0.012	0.002	0.001	0.003	0.002	0.004		0.139	0.348	1.095	2.217	4.269	
GMM		6	0.000	0.000	1.000	0.012	0.002	0.001	0.003	0.002	0.000	0.005	0.140	0.364	1.054	1.827	2.528	4.067

**Table S3.** Results comparing the AERONET bi-lognormal fit, OEV bi-lognormal fits, and GMM fits with 1-6 modes for the 4 dominant aerosol type cases (as in Table S1). The first four rows in each case correspond to the AERONET bi-lognormal fit and the three OEV bi-lognormal fits resulting from obtaining  $r_s$  via minimization of  $s$  and  $R^2$ , as well as their mean.